# Phase Behavior of Solvent Vapor Annealed Thin Films of PS-*b*-P4VP(PDP) Supramolecules

**Wendy van Zoelen,[†] Terhi Asumaa,[‡] Janne Ruokolainen,[‡] Olli Ikkala,[‡] and Gerrit ten Brinke*,[†]**

*Laboratory of Polymer Chemistry, Zernike Institute for Advanced Materials, University of Groningen, Nijenborgh 4, 9747 AG Groningen, The Netherlands, and Department of Engineering Physics and Mathematics and Center for New Materials, Helsinki University of Technology, P.O. Box 2200, FIN-02015 HUT Espoo, Finland*

*Received December 13, 2007; Revised Manuscript Received February 12, 2008*

ABSTRACT: The phase behavior and terrace formation of solvent (chloroform) vapor annealed thin films of asymmetric comb-shaped supramolecules consisting of a polystyrene (PS) block and a supramolecular block of poly(4-vinylpyridine) (P4VP) hydrogen bonded with pentadecylphenol (PDP) on silicon oxide ($SiO_2$) were examined. P4VP(PDP) was found to be present at the $SiO_2$ interface as well as the air interface, implying symmetric boundary conditions. Because of the inherent change in composition by swelling in a selective solvent, the morphology of a lamellar film could be changed to cylindrical by swelling at different vapor pressures of chloroform vapor. Swelling at a specific vapor pressure at the phase boundary between lamellar and cylindrical resulted in noncommon terrace formation behavior. The lowest terrace consisted of two wetting layers forming one lamella, the second terrace contained perpendicular lamellae, and the highest terrace consisted of parallel P4VP(PDP) cylinders. The results are presented in a morphology diagram as a function of film thickness and composition.

## 1. Introduction

In bulk, block copolymers can self-assemble into periodic arrays of different structures, depending on the relative length of the blocks, the molecular weight, and the $\chi$ interaction parameter between the blocks.[1,2] Because of the small periodic length scales involved (typically 10−100 nm), self-assembled block copolymers are interesting candidates for nanotechnology applications. Therefore, the self-assembly of block copolymers is a topic that has received widespread attention over the past decades. The preparation of thin films of highly ordered block copolymers forms the ultimate challenge, as these films can be used to fabricate high-density arrays for microfiltration purposes, data storage, and microelectronics and photonics applications, for example.[3,4] At first, mainly lamellar systems were investigated motivated by the relative simplicity of the corresponding theoretical calculations caused by the symmetry in these systems.[3,5−7] However, as the most interesting applications require perpendicular orientation of cylindrical domains, lately a lot of effort has been devoted into producing such films,[8−16] but also more general studies on the behavior of cylinder-forming block copolymer thin films have been conducted. Besides the pertinent factors applying to ordering in bulk samples, in thin films the interaction of the blocks with the substrate and air interfaces and the film thickness are equally important parameters on which the final microphase-separated structure depends.[17−27] Usually preferential wetting of one of the blocks at an interface leads to a parallel orientation of the microdomains, and when the thickness of the film is incommensurate with the lamellar (or cylindrical/spherical) period, quantization of the film thickness takes place by the formation of terraces.[3,20,27−29] When the interaction with the surface is very strong, a polymer brush may form at the surface. Only when the preferential interaction with the surfaces is reduced, for example by coating a random copolymer brush on a surface, a perpendicular orientation may be achieved.[15,16] When the polymer film is confined between two surfaces, or on the edges of terraces, also perpendicular orientations and interesting nonbulk morphologies such as cylinders with necks or other hybrid structures may occur.[5,23,24,30,31] Furthermore, whereas order in bulk block copolymers is usually induced/improved by annealing at elevated temperatures, order in thin films can also easily be achieved by annealing in solvent vapor. For temperature annealing there might only exist a small window between the highest $T_g$ and the lowest degradation temperature of the components involved, whereas for solvent annealing sufficient mobility is easily induced without the danger of degradation. However, the structures that are obtained in this way do not necessarily correspond to the thermodynamic equilibrium morphology of the solvent free films as the solvent adds more factors on which the final microphase-separated structure depends, such as the nature/selectivity of the solvent,[8,32−36] the solvent evaporation rate,[32,37−39] and the relative solvent vapor pressure.[22,40,41] The effects of these parameters have been observed many times, and although some common behavior in block copolymer thin films has been identified, recently for example Horvat et al. were able to predict the behavior in thin films of cylinder-forming ABA block copolymers quite accurately,[17] it is still difficult to foretell the thin film behavior of a specific system.

In the present paper we report on our study of the phase behavior of two different solvent annealed thin films consisting of supramolecules formed by polystyrene-*block*-poly(4-vinylpyridine) (PS-*b*-P4VP) diblock copolymers hydrogen bonded with pentadecylphenol (PDP) as a function of film thickness and vapor pressure to gain insight into the specific behavior of these comb copolymer thin films. The comb-shaped supramolecules route, where short side chains are attached to one of the blocks of a diblock copolymer by hydrogen bonding, offers as an advantage that the composition of the blocks can be easily adjusted by changing the amount of side chains while using the same block copolymer.[42] This makes it relatively easy to study the effects of solvent swelling on a system that is close to the phase boundary between e.g. lamellar and cylindrical, which is of interest because currently not much is known about

* Corresponding author. E-mail: G.ten.Brinke@rug.nl.
[†] University of Groningen.
[‡] Helsinki University of Technology.

10.1021/ma702780c CCC: $40.75 
Published on Web 04/18/2008

**Table 1. Properties of Polymer Systems Used**

| system | $M_n$(PS), g/mol | $M_n$(P4VP), g/mol | $M_w/M_n$ | PDP/4VP | comb fraction | bulk morphology[50] |
|---|---|---|---|---|---|---|
| P228(PDP)$_{1.5}$ | 301 000 | 19 600 | 1.19 | 1.5 | 0.258 | C |
| P5154(PDP)$_{1.0}$ | 252 000 | 43 000 | 1.09 | 1.0 | 0.399 | L |

the phase behavior of thin films with these compositions. The presence of the side chains itself already induces considerable mobility but, as will be shown, also changes the boundary conditions with the air interface as compared to the pure diblock copolymer.

## 2. Experimental Section

**Materials.** Two different block copolymers of polystyrene and poly(4-vinylpyridine) (PS-*b*-P4VP) were purchased from Polymer Source, Inc., and used as received: P228-S4VP ($M_n$(PS) = 301 000 g/mol, $M_n$(P4VP) = 19 600 g/mol, $M_w/M_n$ = 1.19) and P5154-S4VP ($M_n$(PS) = 252 000 g/mol, $M_n$(P4VP) = 43 000 g/mol, $M_w/M_n$ = 1.09). 3-*n*-Pentadecylphenol (PDP) was purchased from Aldrich and was recrystallized twice from petroleum ether (40−60 w/w) and dried in a vacuum at 40 °C.

**Substrate Preparation.** Silicon (Si) substrates of ∼1 cm$^2$ with a native silicon oxide layer on the surface were cleaned by immersion in a 70/30 v/v piranha solution of concentrated $H_2SO_4$ and $H_2O_2$ (30%) at 60 °C for 1 h, thoroughly rinsed with Milli-Q water, treated ultrasonically in methanol for 15 min, and dried under a stream of nitrogen gas. The substrates were stored in methanol when not immediately used.

**Film Preparation.** PS-*b*-P4VP and PDP (in different stoichiometrical amounts, for details see Table 1) were dissolved in chloroform to yield ∼0.8 wt % solutions. These solutions were spin-coated at speeds between 2000 and 5000 rpm to yield films of the desired thickness (∼80 nm). When thinner films were required, the solutions were diluted before spin-coating. The spin-coated films were exposed to vapors of chloroform ($CHCl_3$) in a glass dish of 7.5 × 5.5 × 3 cm. The dish was typically filled with 60 mL of chloroform while the polymer film was placed on a grating above the solvent. By closing the lid of the dish more or less tightly, the relative solvent vapor pressure inside the dish could roughly be adjusted, resulting in swelling of the films to different swelling ratios. Four different vapor pressures were realized: the lowest pressure P0 when a piece of silicon was placed under the lid, P1 when the lid was closed normally, P2 when some parafilm was wrapped halfway around the lid, and the highest vapor pressure P3 when the lid was completely sealed, resulting in a nearly saturated vapor of chloroform. The swelling ratios, i.e., the ratio between the thickness of the swollen film and the thickness of the original film, at these vapor pressures were roughly determined from the color changes of the films during swelling and varied from 2.5 for P0 to 3 and 3.5 for P1 and P2, respectively, to 4−4.5 times the original thickness for the highest vapor pressure. The thickness of a colored film was estimated using the interference colors of a thin polymer film on silicon (see for example Figure 3.4 of ref 43). After the desired swelling time, the lid of the dish was lifted and the solvent evaporated within a fraction of a second. Samples reached their equilibrium swelling ratio within about 20 min after closing the lid. When needed, PDP was washed from the film by immersing it for 5 min in EtOH, after which the film was blown dry in a stream of nitrogen.

**Characterization.** Atomic force microscopic (AFM) measurements were carried out on a Digital Instruments EnviroScope AFM equipped with a Nanoscope IIIa controller in tapping mode using Veeco RTESPW silicon cantilevers ($f_0$ = 240−296 kHz and $k$ = 20−80 N/m as specified by the manufacturer). AFM images were typically obtained with a scan range of 5 $\mu$m$^2$ and a frequency of 1 Hz/line. Film thicknesses were measured by scratching the film in three different places with a razor blade followed by scanning across the scratch edges. In this case the aspect ratio was 1:8 to minimize distortion along the slow scanning axis due to thermal drift, and background subtraction was accomplished by fitting a plane to the bare substrate, after which the average height of the scanned part was measured.

For transmission electron microscopy (TEM) measurements, films were coated and annealed on freshly cleaved sodium chloride (NaCl) crystals in a similar fashion as on Si. Judging from AFM pictures, the behavior of the systems on $SiO_2$ and NaCl was always identical. After annealing, the films were floated off on deionized water and picked up on a TEM grid. To enhance contrast, the P4VP phase was selectively stained for 3−4 h in vapors of iodine crystals before measuring. Bright-field TEM measurements were performed on a JEOL-1200EX transmission electron microscope operating at an accelerating voltage of 90 kV.

For cross-sectional TEM measurements, the thin films on NaCl were first coated with a layer of carbon, after which a drop of epoxy (Epofix) was put on top. After the epoxy was cured, the NaCl was dissolved and the other side of the film was also coated with carbon, after which the complete epoxy + carbon layer + polymer film + carbon layer assembly was embedded in fresh epoxy and cured at 40 °C overnight. Ultrathin sections (∼70 nm) were microtomed from the embedded specimen using a Leica Ultracut ultramicrotome and a Diatome diamond knife.

## 3. Results and Discussion

To study the influence of solvent swelling on the morphology of thin films of PS-*b*-P4VP(PDP) supramolecules, two different systems were selected. The first one, P228(PDP)$_{1.5}$, has a bulk cylindrical morphology, being situated somewhere in the middle of the hexagonally ordered cylindrical part of the phase diagram. The second system selected, P5154(PDP)$_{1.0}$, has a bulk lamellar morphology but, as will be demonstrated, is not too far from the lamellar/cylindrical border to prevent a solvent-induced lamellar-to-cylindrical morphological transition.

The underlying physics of solvent swelling has recently been well explained by Li and co-workers.[44] When solvent is added to an AB diblock copolymer, the effective interaction parameter will change (whereby it is assumed that $\chi_{AS}$ and $\chi_{BS}$ are not strongly concentration dependent):

$$\chi_{eff} \cong \phi(\chi_{AB} + \Delta\chi) = \phi(\chi_{AB} + |\chi_{AS} - \chi_{BS}|) \qquad (1)$$

where $\phi$ is the volume concentration of copolymer in the solvent and $\Delta\chi$ is the difference between A-solvent and B-solvent interaction parameters $\chi_{AS}$ and $\chi_{BS}$. Upon addition of a neutral solvent, $\Delta\chi \sim 0$ while $\phi$ decreases and thus $\chi_{eff}N$, with $N$ being the total block copolymer length, effectively decreases which may lead the system from an ordered state to a disordered one. This corresponds to a vertical trajectory in the phase diagram as schematically depicted in Figure 1 starting from a lamellar morphology. The effect of addition of a selective solvent is more complicated. If, for instance, an A-selective solvent is added to an AB diblock, then $\Delta\chi > 0$ while $\phi$ decreases (eq 1), which may result in an increase of $\chi_{eff}$ for low swelling degrees when $\Delta\chi$ dominates. For high enough swelling $\phi$ will dominate, resulting in a decrease of $\chi_{eff}$ again.[44] At the same time, selective swelling of the A-block will lead to an increase of the volume fraction of A. This may result in a curved trajectory as is schematically depicted in Figure 1. It now goes without saying that swelling in a selective solvent may change the morphology of the system when a high enough swelling ratio is used. That it can thus be possible to switch a system between different morphologies by adjusting the swelling degree in a partially selective solvent has been proven by Hanley et al. for a polystyrene−polyisoprene block copolymer in bulk,[45,46] recently

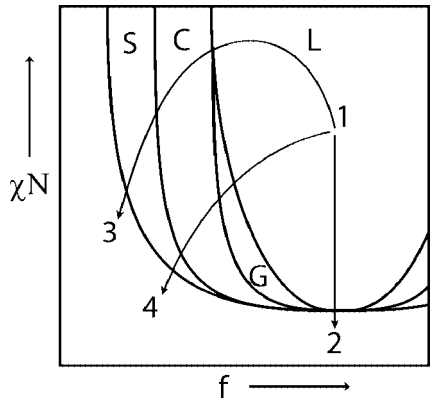


**Figure 1.** Schematic phase diagram showing the effect of swelling in different solvents. Trajectory 1−2 represents swelling in a nonselective solvent; trajectories 1−3 and 1−4 represent swelling in a highly selective and a partially selective solvent, respectively.

by Gong et al. for polystyrene-*block*-poly(methyl methacrylate) (PS-*b*-PMMA) diblock copolymers,[41] and Huang et al. for polystyrene-*block*-polybutadiene-*block*-polystyrene (SBS) triblock copolymers in thin films.[34]

An important observation in relation to the structure formation in thin films of solvent annealed PS-*b*-P4VP(PDP) supramolecules systems concerns the molecular mobility. Because of the presence of PDP, the mobility of PS-*b*-P4VP(PDP) supramolecules is strongly enhanced compared to the pure PS-*b*-P4VP diblock copolymers. PDP is also partly soluble in the PS phase, lowering not only the $T_g$ of P4VP phase but also that of PS.[47] It is this fact that made it actually possible to use the relatively high molecular weight block copolymers that were utilized in this study (Table 1). For pure PS-*b*-P4VP diblock copolymers with these molecular weights and subjected to the vapor pressures employed, significantly longer annealing times would have been necessary to reach equilibrium terrace morphologies.

A final remark concerns the interaction between the different components. From a random copolymer blend miscibility study, the value for the pure PS-*b*-P4VP diblock copolymer was determined to satisfy $0.30 < \chi_{PS\text{-}P4VP} \leq 0.35$ ($T \cong 160$ °C).[48] Very recently, a similar value of $0.317 < \chi_{PS\text{-}P4VP} \leq 0.347$ ($T$ between 160 and 195 °C) was found from a diblock copolymer scattering study.[49] Such a large value implies that PS-*b*-P4VP usually will be in the strong segregation limit already for moderate molar mass values and, hence, can often be swollen in saturated vapor pressures without disordering. The additional presence of PDP, however, effectively lowers the $\chi$ parameter between PS and P4VP. To corroborate the decrease of the $\chi$ parameter, we notice that a gyroid morphology has been found for a PS-*b*-P4VP(PDP)$_{1.0}$ system with a total $M_w$ of 83 300 g/mol, of which the $M_w$ of PS-*b*-P4VP alone was 45 100 g/mol.[50] For the pure diblock copolymer this implies $\chi N \cong 130$. If we assume that $\chi N \leq 60$ for a gyroid phase to be formed, the effective interaction must have been reduced with more than a factor 2 due to the presence of PDP. Therefore, PS-*b*-P4VP(PDP) systems may be in the intermediate segregation regime already for fairly high molecular weights. For the present study this implies that solvent vapor annealing of the supramolecules systems may more easily result in disordering than for the corresponding pure diblock copolymer systems.

**3.1. Swelling of Cylindrical P228(PDP)$_{1.5}$.** *Influence of Film Thickness.* To study the influence of solvent vapor annealing on the morphology in thin films of PS-*b*-P4VP(PDP) supramolecules, we start with the P228(PDP)$_{1.5}$ system. Its bulk morphology consists of hexagonally ordered P4VP(PDP) cylinders in a PS-rich matrix. Such systems are of direct interest to us as these may potentially be used as nanoporous membranes after removal of PDP by simple dissolution.[41] The phrase "PS-rich matrix" is used here because it is well-known from previous studies that a small part of the PDP amphiphiles will reside in the PS domains as well.[48] First, a film of a thickness of ~74 nm was prepared by spin-coating and then annealed in chloroform. Chloroform is usually considered to be a nonselective solvent for *pure* PS-*b*-P4VP, but as the results of this study will demonstrate, this is certainly not the case for PS-*b*-P4VP(PDP) supramolecules. The annealing in chloroform took place at a vapor pressure P1 (see the Experimental Section for a definition of the four different vapor pressures P0, P1, P2, and P3 used) for different periods of time, after which light microscopy images and AFM images were recorded (Figures 2 and 3).[52] Directly after spin-coating, the films appear very rough with striations originating from the center of the film, a well-known effect for films spin-coated from a volatile solvent. Because of the fast solvent evaporation, there is not enough time for structure formation, and the AFM topography image shows a poorly ordered morphology. However, already after 15 min of annealing, the film shows the beginning of terrace formation originating in the thickness variations of the striations, although the topography of the whole film consists of rather disordered short cylinders oriented in different directions. After 1 h, islands can clearly be distinguished, and more importantly, the islands and the lower terrace now exhibit different morphologies. The lower terrace of the film (denoted T1) shows parallel cylinders, whereas the islands (T2) display a hexagonal morphology caused by incommensurability of the cylindrical period with the film thickness. After 4 h of annealing, the film has fully developed islands, and there exists an all-parallel cylindrical morphology; only the edges of islands show a hexagonal morphology. Longer annealing times will only result in rearrangement of the islands due to the Ostwald ripening effect, causing big islands to grow at the expense of the small islands. The time dependence of the mean island size has been extensively studied by Grim et al. for a lamellar PS-*b*-P2VP diblock copolymer and was found to obey a power law $R \propto t^{\alpha}$, with $R$ the mean island size, $t$ the annealing time, and $\alpha$ ranging from 0.12 to 0.26 depending on the surface fraction of islands.[53] Figure 4 shows the TEM pictures of these films. Slight contrast variations indicate that the film was not completely flat, probably

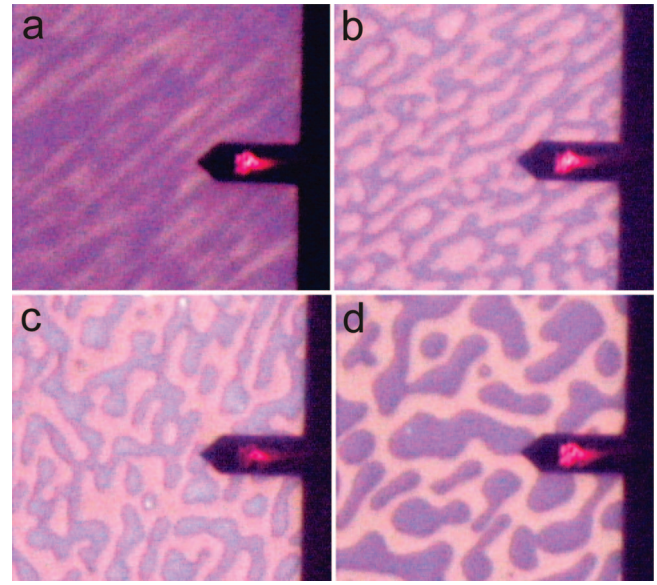


**Figure 2.** Light microscopy images of a 74 nm thin film of P228(PDP)$_{1.5}$ under an AFM tip: (a) directly after spin-coating and swollen at vapor pressure P1 for (b) 15 min, (c) 1 h, and (d) 4 h. The islands appear blue. The dimension of the figures is approximately 280 × 250 $\mu$m$^2$.

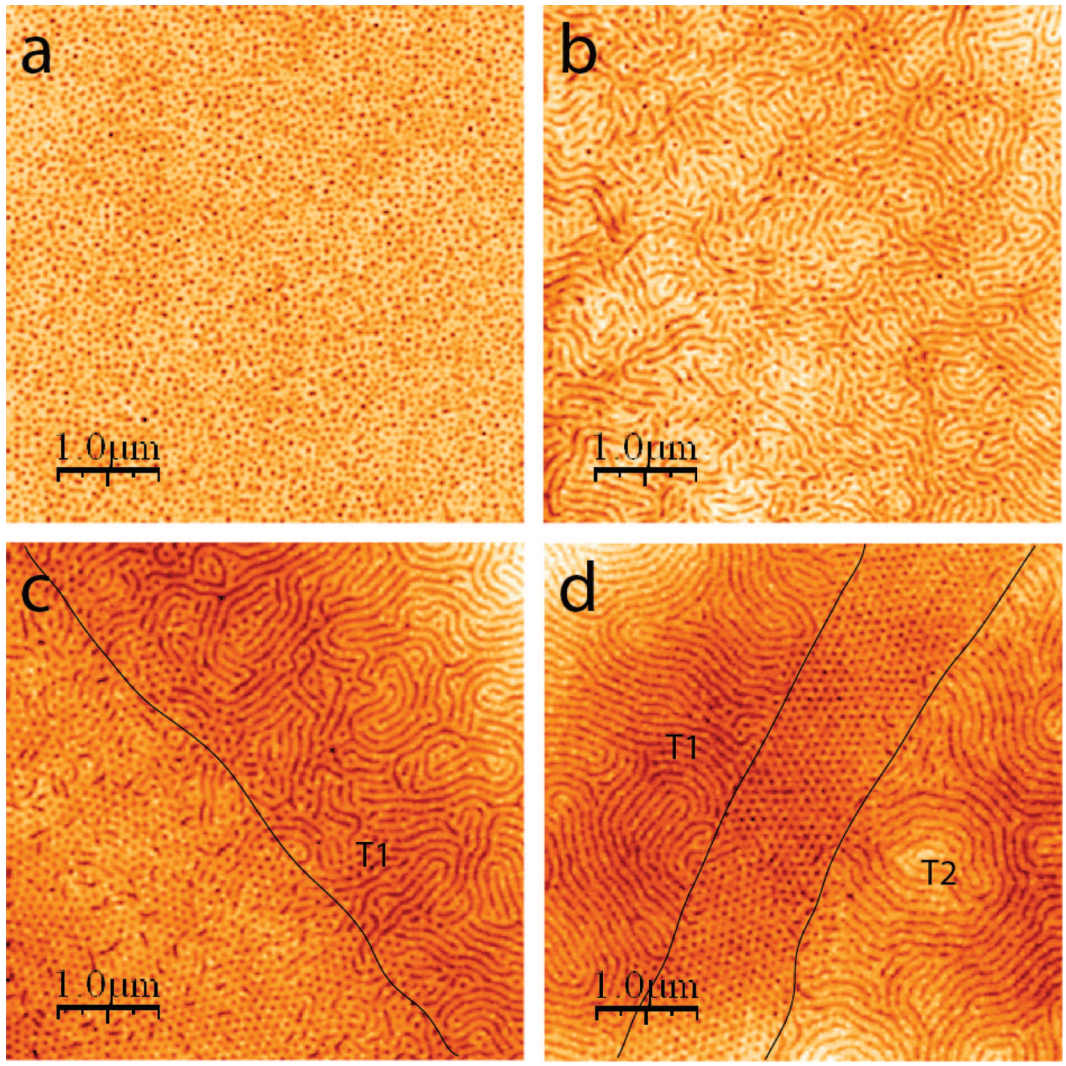


**Figure 3.** Height AFM of a 74 nm thin film of P228(PDP)$_{1.5}$: (a) directly after spin-coating and swollen at vapor pressure P1 for (b) 15 min, (c) 1 h, and (d) 4 h. In (a) $\Delta z \sim 20$ nm and in (b, c, d) $\Delta z \sim 15$ nm. Dark parts correspond to low height values. When terraces were present, pictures were recorded on the edge. For a clear contrast between the cylinders and the matrix images were flattened, hence the lack of visibility of the height difference between the terraces. T1 denotes the lower terrace and T2 the higher terrace.

due to rippling of the film on the TEM grid, and that some cylinders are viewed from an angle. Because of this, it can be concluded that the hexagonal morphology between the islands corresponds to short perpendicularly oriented cylinders. As the crystallization temperature of PDP as well as the $T_g$ of the P4VP(PDP) phase lie around room temperature,[54] the observed holes in the middle of some perpendicular as well as parallel cylinders are likely caused by the formation of small PDP crystallites. In Figure 4a most of this PDP has evaporated in the high vacuum of the TEM, leaving behind a core−shell structure with a clear contrast difference between the PS phase and the hole. The thickness of the terraces was measured as 61.0 ± 0.5 nm for T1 and 87.3 ± 0.3 nm for T2, indicating a cylindrical layer thickness of approximately 87 − 61 = 26 nm.

Subsequently, a thinner film of ~38 nm of P228(PDP)$_{1.5}$ was taken. After annealing in chloroform vapor with the same vapor pressure P1, the behavior observed was similar to that of the thicker films with one important difference. Again T1 terraces with a thickness of 61 nm are formed; however, the transition to the lower terrace in this case is not well ordered hexagonal, and the lower terrace itself (denoted T0) appears featureless, indicating that a lamellar structure is formed at the $SiO_2$ interface (Figure 5). The formation of half-lamellae or brushes is well-known for very thin films of PS-*b*-PVP block copolymers.[42,55–57] PVP, having the highest interfacial energy, will preferentially wet the $SiO_2$ surface, whereas PS will preferentially accumulate at the air interface. The thickness of the lamellar structure formed in our case was measured to be 32.1 ± 0.4 nm. This value is approximately the same as the thickness of one cylindrical layer. In the case of a polymer brush (half-lamellar layer) absorbed on $SiO_2$, the thickness of T0 is expected to be approximately half this value, so that it is very likely that T0 consists of one complete lamellar layer with P4VP(PDP) at both interfaces.

Hence, for PS-*b*-P4VP(PDP) supramolecules different boundary conditions apply as compared to the pure diblock copolymer. As an amphiphile, PDP probably has a strong preference for the air interface, and as P4VP hydrogen bonds with PDP, the air interface is now preferential toward P4VP(PDP) so that symmetric boundary conditions apply, leading to the terrace morphology summarized in Figure 6. This morphology closely resembles the morphology found for a free-standing film of an asymmetric poly(styrene-*b*-butadiene) diblock copolymer.[25] Theoretical calculations for asymmetric block copolymers, where also symmetric wetting conditions apply and both surfaces are attractive toward the minority block, also predict such behavior.[17,19] The surface layer is transformed to a more planar morphology as the average mean curvature is decreased in order to adapt to the planar symmetry of the interface. Of course, the cylindrical structure that is observed in the higher terraces T1

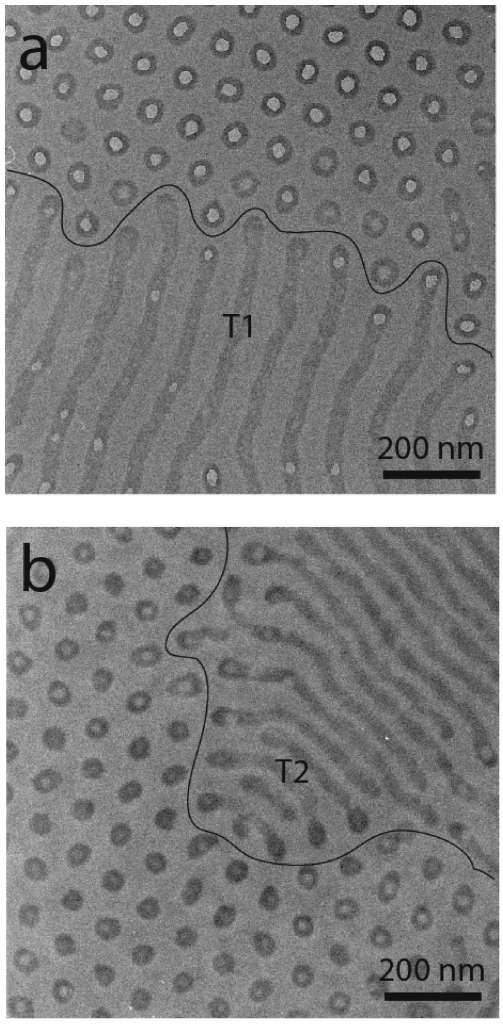


**Figure 4.** TEM of thin films of P228(PDP)$_{1.5}$ on NaCl after 4 h of annealing at vapor pressure P1: (a) a single layer of parallel cylinders (T1) next to transitional perpendicular cylinders; (b) a double layer of parallel cylinders (T2) next to perpendicular cylinders. Holes in the middle of perpendicular as well as parallel cylinders are likely caused by crystallization and, in the case of a clear contrast difference between the hole and the PS phase, evaporation of PDP.

and T2 is extremely collapsed due to the fast solvent evaporation. The cylindrical period of ~90 nm in the AFM images indicates a distance between layers of cylinders of 90 × sin(60) = 78 nm during swelling. This indicates a swelling degree of ≅78/26 = 3, which is in accordance with the observed color changes that occurred during swelling.

*Influence of Vapor Pressure.* The vapor pressure dependence of the structure formation in the cylindrical thin films has been explored by annealing the ~74 nm P228(PDP)$_{1.5}$ films for 15 min at different vapor pressures P0, P1, P2, and P3. Figure 7a shows a film annealed at P0. At this low vapor pressure only disordered micelles, occasionally growing into cylinders, and no distinct terrace formation can be seen, all indicating that the system is not mobile enough to form an ordered morphology within the 15 min that were used. The result of 15 min of annealing at P1 can be recalled from Figure 3b, where already clear structure and terrace formation could be observed after this time, although all terraces showed the same morphology. For P2, the terraces already display different morphologies, and finally, annealing at the highest vapor pressure P3 results in a smooth surface without a well-ordered morphology, much like the topography image directly after spin-coating. Apparently, for this amount of chloroform a disordered state is formed during annealing, which results in a poorly ordered microphase-separated morphology after the fast evaporation of chloroform, comparable to the structure formation from the dilute spin-coating solution.

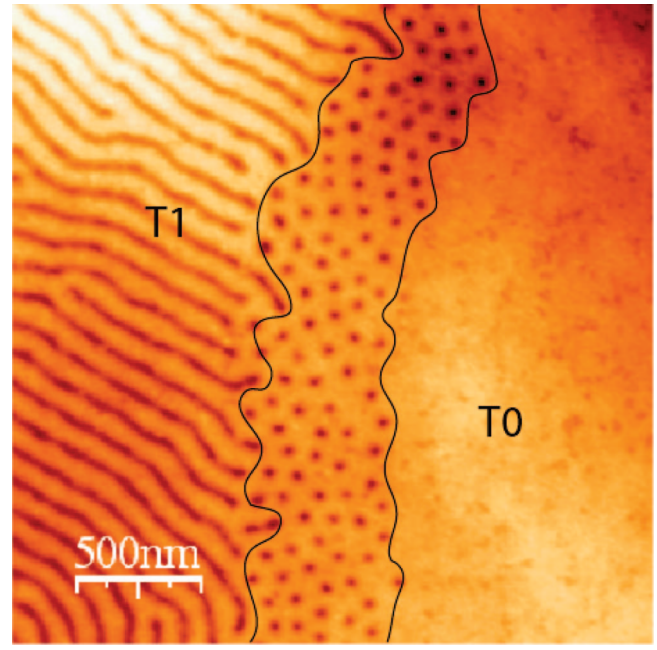


**Figure 5.** Height AFM of a ~38 nm P228(PDP)$_{1.5}$ film after annealing at vapor pressure P1 for 4 h showing a transition from the first cylindrical layer (T1) to a featureless structure (T0). $\Delta z \sim 20$ nm; dark parts correspond to low height values.

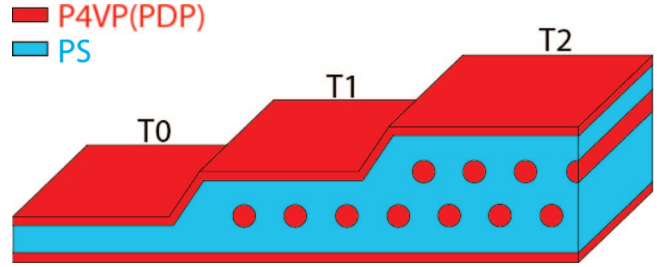


**Figure 6.** Schematic picture of the terrace morphology of P228(PDP)$_{1.5}$ thin films.

At low solvent concentrations such as P0, the mobility is low, and the formation of the equilibrium structure will take longer than at high concentrations. However, although the terraces did not reach their equilibrium terrace morphology at these short annealing times, the systems showed a tendency to form parallel cylinders at all vapor pressures except P3. Recently, Cavicchi and co-workers also varied the solvent concentration of chloroform in a polyisoprene-*block*-polylactide diblock copolymer thin film and found perpendicular cylinders for higher solvent concentrations.[40] In their case, however, the solvent could mediate the interfacial interactions to make the air interface less selective to either block, which is different from our case, where the preferential interaction of P4VP(PDP) with the air interface is stronger than a possible solvent effect on the interfacial interactions.

Furthermore, a spherical morphology was never observed in the P228(PDP)$_{1.5}$ system, indicating that the system does not exhibit an order−order transition (OOT) between cylinders and spheres during swelling in chloroform and that there the system crosses a direct boundary between the cylindrical and the disordered state. Although this boundary is very small in a theoretical phase diagram, it is not uncommon in experimental systems; e.g., it was found to exist over a large window for diblock copolymers of polystyrene and polyisoprene.[45]

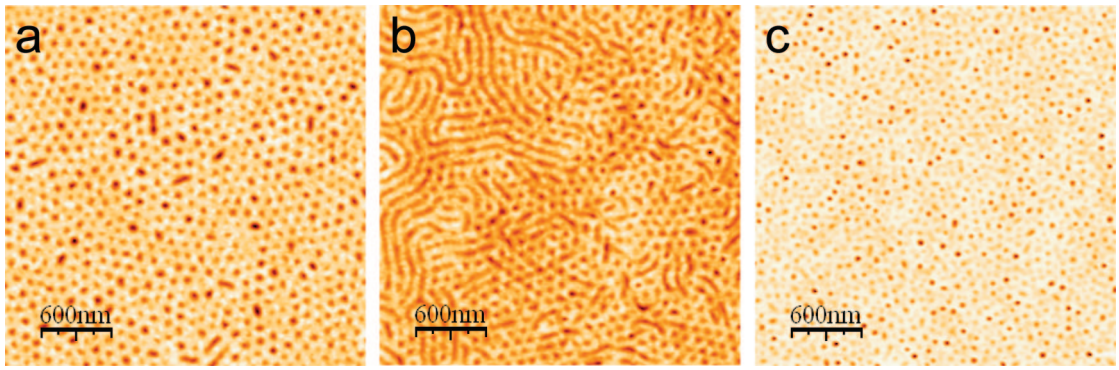


**Figure 7.** Height AFM of a 74 nm thin film of P228(PDP)$_{1.5}$ swollen for 15 min at vapor pressures: (a) P0, (b) P2, and (c) P3. In (a, b) $\Delta z \sim 15$ nm and in (c) $\Delta z \sim 30$ nm. Dark parts correspond to low height values.

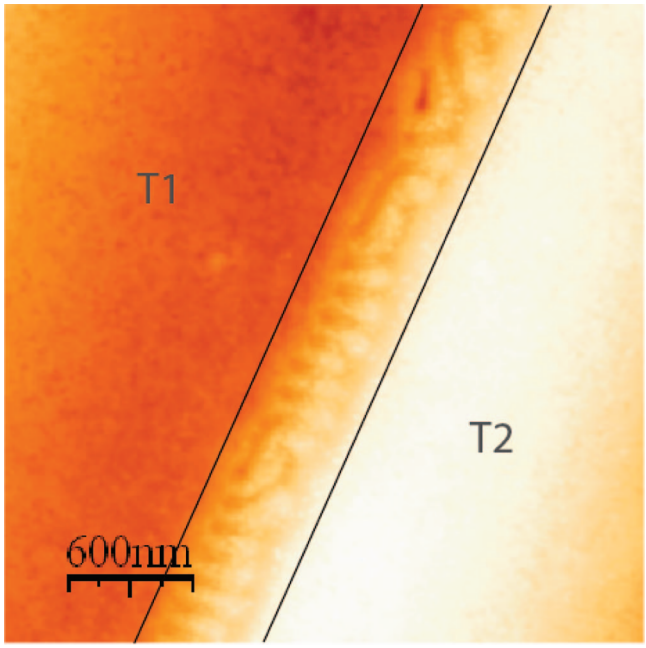


**Figure 8.** Height AFM of P5154(PDP)$_{1.0}$ after 21 h annealing at vapor pressure P0. $\Delta z \sim 30$ nm; dark parts correspond to low height values.

**3.2. Swelling of Lamellar P5154(PDP)$_{1.0}$.** After having studied the behavior of a completely cylindrical system, the use of a system with a higher weight fraction of the P4VP(PDP) comb made it possible to study the thin film behavior at an OOT between lamellae and cylinders, as the final results will show. Figure 8 shows the morphology of the bulk lamellar system P5154(PDP)$_{1.0}$ after 21 h of annealing at P0. At this low vapor pressure, the structure clearly consists of parallel lamellae, with some perpendicular lamellae at the edge of the terraces. Figure 9 shows the morphology after 1 and 24 h of annealing at P1. At first sight the morphologies of T1 and T2 appear to be cylindrical; however, even after short annealing times at P1, a hexagonal structure indicating perpendicular cylinders was never observed. Together with the absence of any perpendicular cylinders at the terrace edges, this suggests that the structure observed might not be simply cylindrical. Figure 10 shows a TEM picture of the system, where it can be clearly seen that T2 consists of two layers of cylinders, which smoothly transform into the structure of T1, where the P4VP(PDP) domains seem to be somewhat wider than for the cylinders in T2. In cross-sectional TEM images (Figure 11) the two wetting layers forming a lamella in the lowest terrace are now clearly visible. However, the structure in T1 does not seem to differ much from the cylinders in the higher terraces. To study this in more detail, AFM images of the surface structures were taken after washing away PDP (Figure 12). Now, the difference between T1 and T2 is very obvious, as the AFM tip can enter the surface of T1 much deeper. These differences can be explained by assuming that T1 consists of perpendicular lamellae, shielded from the surfaces by two wetting layers, leading to the terrace morphology depicted in Figure 13. The perpendicular lamellae are very short and barely distinguishable from cylinders but have an important difference in chain distribution. During flushing with ethanol to wash away PDP, the polymer chains on the surface will rearrange, causing deep valleys in the lamellar structure. In the case of our cylindrical thin films where a wetting layer is always present, the P4VP(PDP) cylinders are shielded from the surface by two layers of PS blocks that cannot be easily penetrated, and only the PDP from the surface will be washed away (Figure 14). The only height contrast in the AFM pictures of cylinders is caused by the AFM tip being able to compress the soft P4VP(PDP) domains.

Perpendicular lamellae are well-known to form for thin films where the film thickness of a confined film is incommensurate with the lamellar period. However, when a film has enough freedom to form terraces, it will generally form an all parallel morphology. A seemingly stable terrace of perpendicular lamellae, even though shielded from the surface by a wetting layer, to the best of our knowledge, has not been observed before.

An explanation for this unusual behavior can be found by looking at the structure of P5154(PDP)$_{1.0}$ annealed at a lower vapor pressure P0 (Figure 8) and a higher vapor pressure P2 (Figure 15). As mentioned before, at a lower vapor pressure P0, the structure clearly consists of parallel lamellae, whereas at the higher vapor pressure P2, the system forms some perpendicular cylinders. This proves that the system is near the phase boundary when swollen at P1. In a thin film, the final morphology of a terrace is a result of the interplay between the composition of the polymer and the surface field. The surface fields extend into the bulk with a decay length of about one to one and a half microdomain spacing, and they are additive, meaning that for very thin films the effects of both surfaces combine.[17] That is why theoretically, for cylindrical $A_3B_{12}A_3$ triblock films with a thickness of up to 3 times the natural layer thickness and a strongly A attractive surface, the inner structure of the film was found to be reconstructed to form two layers of perforated lamellae, with a wetting layer near the surfaces.[17] For thicker films the surface fields do not combine that strong anymore, and the inner structure takes the bulk (parallel) cylindrical form. For a slightly weaker surface field, the transition from perforated lamellae to cylinders within the film occurs earlier, and the perforated lamellar phase can only be found in the middle of a film with a thickness of 2 times the

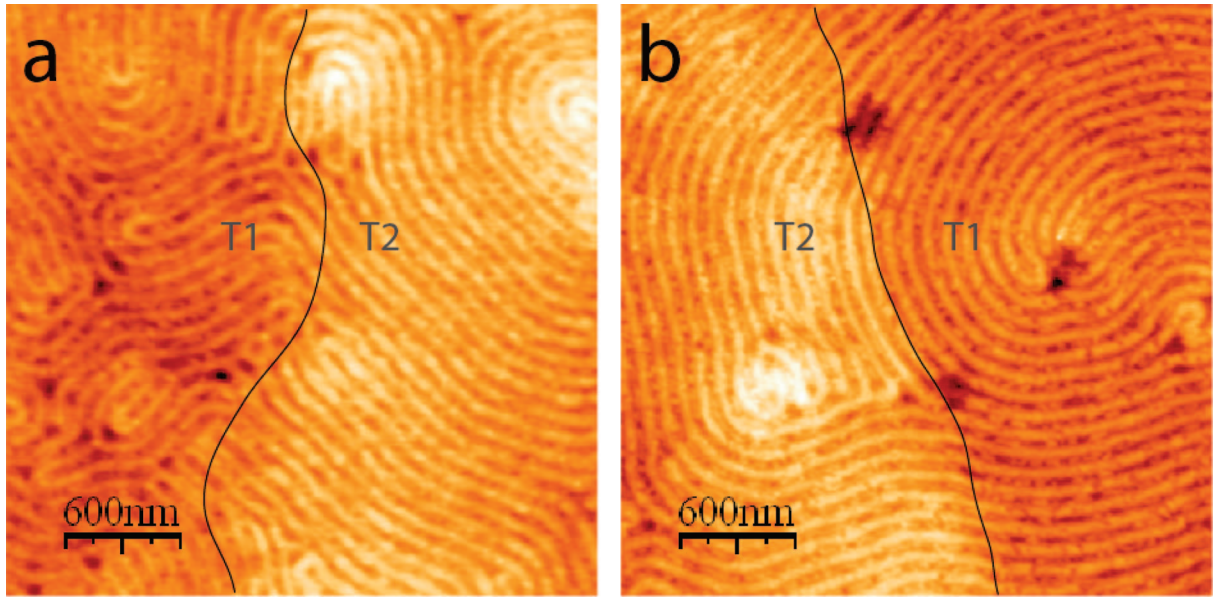


**Figure 9.** Height AFM of P5154(PDP)$_{1.0}$ after (a) 1 and (b) 24 h of annealing at vapor pressure P1. $\Delta z \sim 15$ nm; dark parts correspond to low height values.

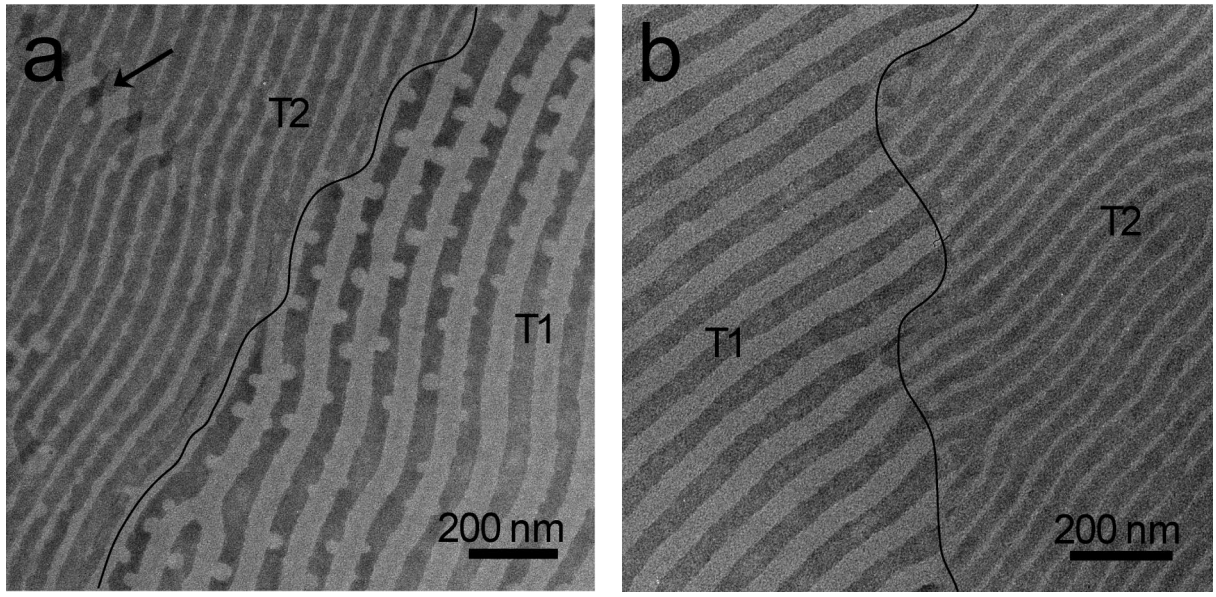


**Figure 10.** TEM of 18 h annealed P5154(PDP)$_{1.0}$ sample at vapor pressure P1. Holes in the P4VP(PDP) phase in (a) are again caused by crystallization of PDP. The arrow points to a defect where a cylinder in the top layer crosses a cylinder on the bottom layer.

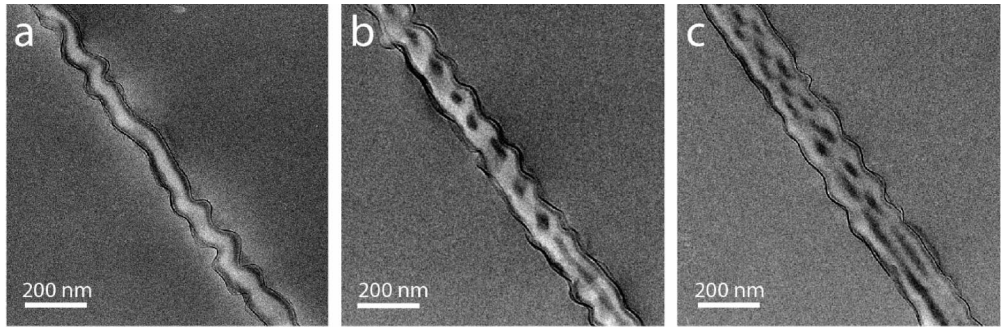


**Figure 11.** TEM of P5154(PDP)$_{1.0}$ cross sections: (a) two wetting layers forming a lamella in T0; (b) the cross-sectional structure of T1; (c) T2 and T3, two and three layers of cylinders.

natural layer thickness. Finally, for more weaker (more strongly B attractive) surface fields, the structure of the surface changes, from a wetting layer, to perpendicular cylinders, to parallel cylinders, to perforated lamellae, and finally to lamellae for a strongly B attractive surface, while the inner structure remains parallel cylinders (see Figure 8 of ref 17). Although these

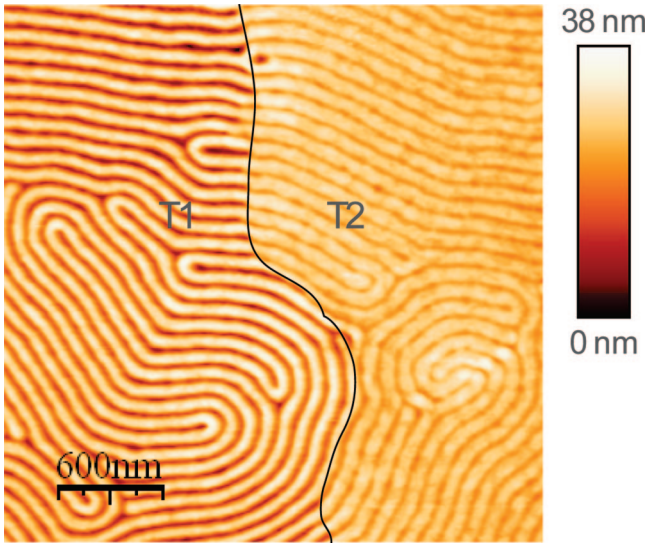


**Figure 12.** Height AFM of P5154(PDP)$_{1.0}$ after 24 h of annealing at vapor pressure P1, washed with ethanol.

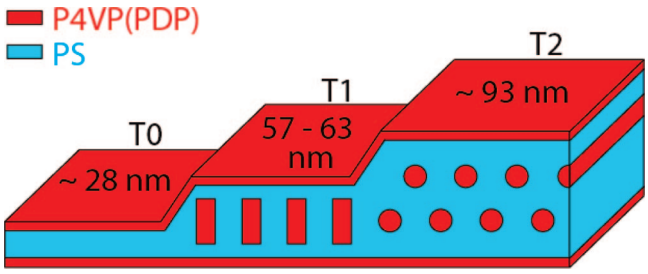


**Figure 13.** Schematic drawing of the terrace morphology of P5154-(PDP)$_{1.0}$ at vapor pressure P1.

calculations were done for a triblock, they were proven to qualitatively apply equally well for an AB diblock. However, the calculations concerned the intermediate segregation regime ($\chi N \cong 35$), whereas in our case, we are dealing with a more strongly segregated system, where the formation of a perforated lamellar phase is not obvious and the surface field might be expected to drive a system directly from lamellar to cylindrical. This assumption is supported by the fact that for thin films of PS-*b*-P4VP(PDP) with a lower molecular weight, where intermediate segregation applies, hexagonally perforated lamellar phases have indeed been found.[58]

For a very thin film (T0), the combined effect of the preferential interaction of both the $SiO_2$ and the air interface with P4VP(PDP) causes the structure to be lamellar (two wetting layers) for both comb copolymer systems used in this study; nevertheless, for the thicker films (T1 and T2), the surface field is diminished enough to allow the system to adopt its "bulk" structure in the middle of the film, with a half-lamellar wetting layer at both surfaces. However, as the composition of the P5154(PDP)$_{1.0}$ system is on the edge between lamellar and cylindrical for the vapor pressure P1, we now have to take into account not only the surface field but also the composition of the system. Figure 16 shows a schematic morphology diagram for the swollen P5154(PDP)$_{1.0}$ system near the borderline between a lamellar and cylindrical morphology as it follows from all these observations. In this diagram the surface morphologies are given as a function of the layer thickness $t/L_0$ and the volume fraction of PS, $f_{PS}$, which in our case can be altered by changing the chloroform vapor pressure according to Figure 1. Only the small window of $f_{PS}$ that is near the cylindrical/lamellar phase boundary is represented. As the system is in the strong segregation regime for low enough vapor pressures, only parallel cylinders and lamellae are expected to form stable terraces. Furthermore, as both surfaces are very strongly attractive toward the P4VP(PDP) block, a wetting layer is always present. The wetting layers effectively screen the surface field, and the films can also be regarded as being one layer thinner and trapped between two slightly weaker PS attractive surfaces. The surface field also causes the asymmetry in the system; there for thinner films, where the surface fields interact more strongly, the system will be driven toward a planar geometry at lower volume fractions than for thicker films. For a higher volume fraction of the PS block (in our case accomplished by a higher $CHCl_3$ vapor pressure, see Figure 1), the cylindrical form evidently becomes more stable than the lamellar form; however, at the boundary between the two stable phases, at a layer thickness of about 2 times the equilibrium layer thickness, possibly neither parallel cylinders nor parallel lamellae may be stable, and the system will form perpendicular lamellae or cylinders. In the case of swelling at P1 only perpendicular cylinders are stable, but swelling at P2 shifts the volume fraction $f_{PS}$ slightly to the right, where both perpendicular cylinders and lamellae are stable (an assumption supported by Figure 15). Films with this thickness are expected to form terraces with a thickness of 1 and 3 times the layer thickness; however, the perpendicular structure may be kinetically trapped due to the large height difference between the two terraces. This suggests that the morphology we found for T1 is only a long-lived metastable state, which is corroborated by the height that was measured for the different terraces: T0 and T2 were measured to be 27.6 ± 0.1 and 92.8 ± 0.7 nm, respectively, yet the value for T1 ranged from 57 to 63 nm depending on the original film thickness. Furthermore, it was tried to swell the system at higher vapor pressures to obtain a completely cylindrical morphology; however, this was not successful. The morphology did become cylindrical; however, the structure contained a high amount of defects in the form of interconnections between neighboring cylinders. This might be caused by the fact that at higher vapor pressures $\chi_{PS\text{-}P4VP,eff}$ was low enough for the system to be in the intermediate or weak segregation regime. As the system was on the edge between lamellar and cylindrical and maybe even almost disordered, the structure might be a kind of badly ordered interconnected structure. Furthermore, it was difficult to obtain a repeatable vapor pressure in the region between P2 and P3 in our setup. As the morphology at higher vapor pressures is likely to be more strongly dependent on the vapor pressure, obtaining reproducible results in this regime was not straightforward.

## 4. Conclusion

The thin film behavior of high molecular weight asymmetric PS-*b*-P4VP(PDP) comb-shaped supramolecules on silicon oxide annealed in chloroform was investigated. As opposed to the pure PS-*b*-P4VP diblock, where PS segregates at the air interface due to the low surface energy of PS, in the case of PS-*b*-P4VP(PDP), P4VP(PDP) segregates at the air interface due to the preferential interaction of the amphiphile PDP with the air interface, which results in symmetric boundary conditions. Because of the presence of PDP, which can be considered to be a highly selective solvent toward P4VP, the systems are extremely mobile as compared to the pure diblock copolymer and also the effective $\chi$ parameter between PS and P4VP is lowered. Nevertheless, at low enough vapor pressures, the systems were still considered to be in the strong segregation regime. It was found that a bulk lamellar system with a composition close to the lamellar/cylindrical border could be switched between these two different morphologies, depending on the solvent vapor pressure of the partially PS selective solvent chloroform. Swelling of this system at a specific vapor pressure

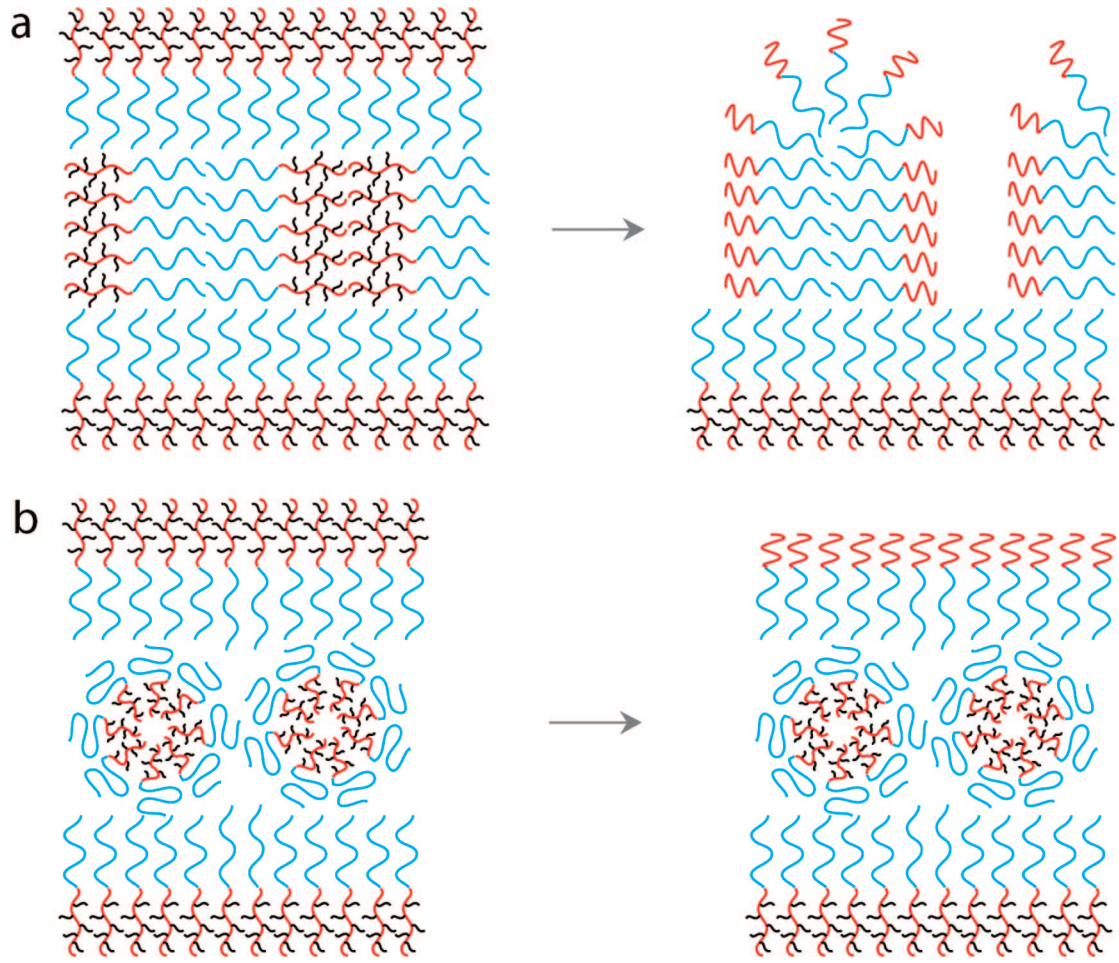


**Figure 14.** Rearrangement of the surface chains after washing away PDP in (a) perpendicular lamellar PS-*b*-P4VP(PDP) and (b) parallel cylindrical PS-*b*-P4VP(PDP). The cylinders are shielded by a double layer of PS blocks, leaving the ethanol unable to enter and wash away PDP from within the cylinders.

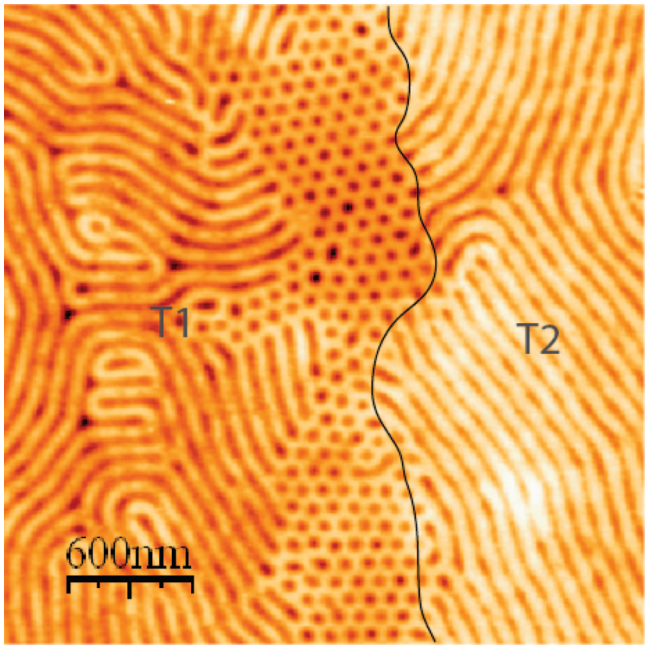


**Figure 15.** Height AFM of P5154(PDP)$_{1.0}$ after 17 h of annealing at vapor pressure P2. $\Delta z \sim 15$ nm; dark parts correspond to low height values.

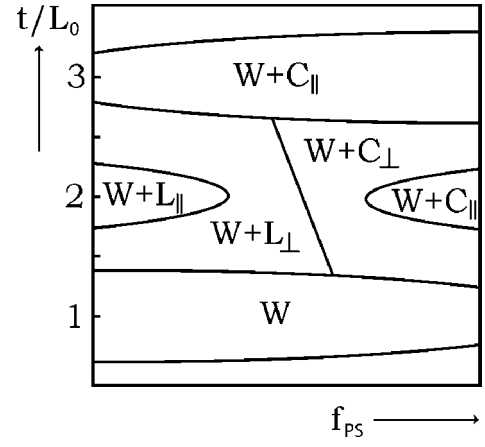


**Figure 16.** Qualitative phase diagram of surface reconstructions for a strongly segregated diblock copolymer near an L−C phase boundary at a fixed (P4VP(PDP) attractive) surface field as a function of the number of layers $t/L_0$ and the volume fraction of the PS block $f_{PS}$. W represents a wetting layer; $C_\perp$ ($L_\perp$) and $C_{||}$ ($L_{||}$) symbolize perpendicular and parallel cylinders (lamellae), respectively. The diagram represents only a small part of the total phase diagram where $f_{PS}$ is near the lamellar/cylindrical border. For smaller $f_{PS}$ values the diagram obviously only contains lamellae, whereas for higher values only cylinders are stable.

resulted in terraces of metastable perpendicular lamellae and parallel cylinders in a single film. This was attributed to the fact that the composition of the system was at a phase boundary between lamellar and cylindrical at the used vapor pressure. The influence of the surface field could shift the structure of

thinner films toward a more planar morphology, and as the system was most likely strongly segregated, this resulted in perpendicular lamellae instead of an intermediate perforated lamellar structure. This behavior should not necessarily be specific to our PS-*b*-P4VP(PDP) supramolecules and may also apply to other strongly segregated block copolymer systems. Finally, the results were summarized in a phase diagram (Figure 16).

**Acknowledgment.** We thank Prof. Robert Magerle from the Chemnitz University of Technology for helpful discussions on block copolymer thin films. Ari Laiho from the Helsinki University of Technology is greatly acknowledged for his advice on preparing cross-sectional TEM pictures. This work was financially supported by the European Commission project COMPOSE (project number NMP3-CT-2003-505633) and The Netherlands Organisation for Scientific Research (NWO).

## References and Notes

(1) Hamley, I. W. *The Physics of Block Copolymers*; Oxford Science Publications: Oxford, 1998.
(2) Matsen, M. W.; Bates, F. S. *Macromolecules* **1996**, *29*, 1091–1098.
(3) Fasolka, M. J.; Mayes, A. M. *Annu. Rev. Mater. Res.* **2001**, *31*, 323–355.
(4) Segalman, R. A. *Mater. Sci. Eng. R* **2005**, *48*, 191–226.
(5) Fasolka, M. J.; Banerjee, P.; Mayes, A. M.; Pickett, G.; Balazs, A. C. *Macromolecules* **2000**, *33*, 5702–5712.
(6) Walton, D. G.; Kellogg, G. J.; Mayes, A. M.; Lambooy, P.; Russell, T. P. *Macromolecules* **1994**, *27*, 6225–6228.
(7) Anastasiadis, S. H.; Russell, T. P.; Satija, S. K.; Majkrzak, C. F. *Phys. Rev. Lett.* **1989**, *62*, 1852–1855.
(8) Cavicchi, K. A.; Berthiaume, K. J.; Russell, T. P. *Polymer* **2005**, *46*, 11635–11639.
(9) Kim, S.; Briber, R. M.; Karim, A.; Jones, R. L.; Kim, H.-C. *Macromolecules* **2007**, *40*, 4102–4105.
(10) Kim, S. H.; Misner, M. J.; Yang, L.; Gang, O.; Ocko, B. M.; Russell, T. P. *Macromolecules* **2006**, *39*, 8473–8479.
(11) Kim, S. H.; Misner, M. J.; Xu, T.; Kimura, M.; Russell, T. P. *Adv. Mater.* **2004**, *16*, 226–231.
(12) Kim, S. H.; Misner, M. J.; Russell, T. P. *Adv. Mater.* **2004**, *16*, 2119–2123.
(13) Kitano, H.; Akasaka, S.; Inoue, T.; Chen, F.; Takenaka, M.; Hasegawa, H.; Yoshida, H.; Nagano, H. *Langmuir* **2007**, *23*, 6404–6410.
(14) Olayo-Valles, R.; Guo, S.; Lun, M. S.; Leighton, C.; Hillmyer, M. A. *Macromolecules* **2005**, *38*, 10101–10108.
(15) Thurn-Albrecht, T.; Steiner, R.; DeRouchey, J.; Stafford, C. M.; Huang, E.; Bal, M.; Tuominen, M.; Hawker, C. J.; Russell, T. P. *Adv. Mater.* **2000**, *12*, 787–791.
(16) Mansky, P.; Liu, Y.; Huang, E.; Russell, T. P.; Hawker, C. *Science* **1997**, *275*, 1458–1460.
(17) Horvat, A.; Lyakhova, K. S.; Sevink, G. J. A.; Zvelindovsky, A. V.; Magerle, R. *J. Chem. Phys.* **2004**, *120*, 1117–1126.
(18) Lyakhova, K. S.; Sevink, G. J. A.; Zvelindovsky, A. V.; Horvat, A.; Magerle, R. *J. Chem. Phys.* **2004**, *120*, 1127–1137.
(19) Huinink, H. P.; Brokken-Zijp, J. C. M.; van Dijk, M. A.; Sevink, G. J. A. *J. Chem. Phys.* **2000**, *112*, 2452–2462.
(20) Kim, H.-C.; Russell, T. P. *J. Polym. Sci., Part B* **2001**, *39*, 663–668.
(21) Knoll, A.; Tsarkova, L.; Krausch, G. *Nano Lett.* **2007**, *7*, 843–846.
(22) Knoll, A.; Horvat, A.; Lyakhova, K. S.; Krausch, G.; Sevink, G. J. A.; Zvelindovsky, A. V.; Magerle, R. *Phys. Rev. Lett.* **2002**, *89*, 035501.
(23) Krausch, G.; Magerle, R. *Adv. Mater.* **2002**, *14*, 1579–1583.
(24) Lyakhova, K. S.; Horvat, A.; Zvelindovsky, A. V.; Sevink, G. J. A. *Langmuir* **2006**, *22*, 5848–5855.
(25) Radzilowski, L. H.; Carvalho, B. L.; Thomas, E. L. *J. Polym. Sci., Part B* **1996**, *34*, 3081–3093.
(26) Sivaniah, E.; Hayashi, Y.; Matsubara, S.; Kiyono, S.; Hashimoto, T.; Fukunaga, K.; Kramer, E. J.; Mates, T. *Macromolecules* **2005**, *38*, 1837–1849.
(27) Tsarkova, L.; Knoll, A.; Krausch, G.; Magerle, R. *Macromolecules* **2006**, *39*, 3608–3615.
(28) van Dijk, M. A.; van den Berg, R. *Macromolecules* **1995**, *28*, 6773–6778.
(29) Henkee, C. S.; Thomas, E. L.; Fetters, L. J. *J. Mater. Sci.* **1988**, *23*, 1685–1694.
(30) Konrad, M.; Knoll, A.; Krausch, G.; Magerle, R. *Macromolecules* **2000**, *33*, 5518–5523.
(31) Yin, Y.; Sun, P.; Jiang, R.; Li, B.; Chen, T.; Jin, Q.; Ding, D.; Shi, A.-C. *J. Chem. Phys.* **2006**, *124*, 184708.
(32) Cong, Y.; Zhang, Z.; Fu, J.; Li, J.; Han, Y. *Polymer* **2005**, *46*, 5377–5384.
(33) Elbs, H.; Drummer, C.; Abetz, V.; Krausch, G. *Macromolecules* **2002**, *35*, 5570–5577.
(34) Huang, H.; Hu, Z.; Chen, Y.; Zhang, F.; Gong, Y.; He, T. *Macromolecules* **2004**, *37*, 6523–6530.
(35) Peng, J.; Xuan, Y.; Wang, H.; Yang, Y.; Li, B.; Han, Y. *J. Chem. Phys.* **2004**, *120*, 11163.
(36) Tokarev, I.; Krenek, R.; Burkov, Y.; Schmeisser, D.; Sidorenko, A.; Minko, S.; Stamm, M. *Macromolecules* **2005**, *38*, 507–516.
(37) Gong, Y.; Hu, Z.; Chen, Y.; Huang, H.; He, T. *Langmuir* **2005**, *21*, 11870–11877.
(38) Kim, G.; Libera, M. *Macromolecules* **1998**, *31*, 2569–2577.
(39) Zhang, Q.; Tsui, O. K. C.; Du, B.; Zhang, F.; Tang, T.; He, T. *Macromolecules* **2000**, *33*, 9561–9567.
(40) Cavicchi, K. A.; Russell, T. P. *Macromolecules* **2007**, *40*, 1181–1186.
(41) Gong, Y.; Huang, H.; Hu, Z.; Chen, Y.; Chen, D.; Wang, Z.; He, T. *Macromolecules* **2006**, *39*, 3369–3376.
(42) Zhao, J.; Tian, S.; Wang, Q.; Liu, X.; Jiang, S.; Ji, X.; An, L.; Jiang, B. *Eur. Phys. J. E* **2005**, *16*, 49–56.
(43) http://irs.ub.rug.nl/ppn/291147801.
(44) Li, Y.; Wang, X.; Sanchez, I. C.; Johnston, K. P.; Green, P. F. *J. Phys. Chem. B* **2007**, *111*, 16–25.
(45) Hanley, K. J.; Lodge, T. P.; Huang, C.-I. *Macromolecules* **2000**, *33*, 5918–5931.
(46) Hanley, K. J.; Lodge, T. P. *J. Polym. Sci., Part B* **1998**, *36*, 3101–3113.
(47) van Zoelen, W.; Alberda van Ekenstein, G.; Ikkala, O.; ten Brinke, G. *Macromolecules* **2006**, *39*, 6574–6579.
(48) Alberda van Ekenstein, G. O. R.; Meyboom, R.; ten Brinke, G.; Ikkala, O. *Macromolecules* **2000**, *33*, 3752–3756.
(49) Zha, W.; Han, C. D.; Lee, D. H.; Han, S. H.; Kim, J. K.; Kang, J. H.; Park, C. *Macromolecules* **2007**, *40*, 2109–2119.
(50) Valkama, S.; Ruotsalainen, T.; Nykänen, A.; Laiho, A.; Kosonen, H.; ten Brinke, G.; Ikkala, O.; Ruokolainen, J. *Macromolecules* **2006**, *39*, 9327–9336.
(51) Ikkala, O.; ten Brinke, G. *Science* **2002**, *295*, 2407–2409.
(52) All AFM images in this article were treated with flattening or plane fit filters to increase visibility of the microdomain structures. Therefore, the height ranges of the color scales do not correspond to the terrace heights.
(53) Grim, P. C. M.; Nyrkova, I. A.; Semenov, A. N.; ten Brinke, G.; Hadziiouannou, G. *Macromolecules* **1995**, *28*, 7501–7513.
(54) Luyten, M. C.; Alberda van Ekenstein, G. O. R.; ten Brinke, G.; Ruokolainen, J.; Ikkala, O.; Torkkeli, M.; Serimaa, R. *Macromolecules* **1999**, *32*, 4404–4410.
(55) Li, X.; Peng, J.; Wen, Y.; Kim, D. H.; Knoll, W. *Polymer* **2007**, *48*, 2434–2443.
(56) Liu, Y.; Zhao, W.; Zheng, X.; King, A.; Singh, A.; Rafailovich, M. H.; Sokolov, J.; Dai, K. H.; Kramer, E. J.; Schwarz, S. A.; Gebizlioglu, O.; Sinha, S. K. *Macromolecules* **1994**, *27*, 4000–4010.
(57) Spatz, J. P.; Möller, M.; Noeske, M.; Behm, R. J.; Pietralla, M. *Macromolecules* **1997**, *30*, 3874–3880.
(58) Unpublished results.

MA702780C